MEASUREMENT OF INTERFACE PRESSURE IN INTERFERENCE FITS

R. LEWIS*, M.B. MARSHALL, R.S. DWYER-JOYCE

Department of Mechanical Engineering, University of Sheffield, Mappin Street, S1 3JD
*Corresponding author

ABSTRACT

When components such as bearings or gears are pressed onto a shaft the resulting interference induces a pressure at the interface. The size of this pressure is important as many components fail because fatigue initiates from press-fit stress concentrations. This aim of this work was to develop ultrasound as a tool to non-destructively determine press-fit contact pressures.

An interference fit interface behaves like a spring. If the pressure is high there are few air gaps; so it is very stiff and allows transmission of an ultrasonic wave. If the pressure is low then interface stiffness is lower and most ultrasound is reflected. A *spring model* was used to determine maps of contact stiffness from interference fit ultrasonic reflection data. A calibration procedure was then used to determine the pressure.

The interface contact pressure has been determined for a number of different press and shrink fit cases. The results show a central region of approximately uniform pressure with edge stress at the contact sides. The magnitude of the pressure in the central region agrees well with the elastic Lamé analysis. In the more severe press fit cases, the surfaces scuffed which lead to anomalies in the reflected ultrasound. These anomalies were associated with regions of surface damage at the interface.

The average contact pressure in a shrink fit and press fit joint were similar. However in the shrink fit joint more uneven contact pressure was observed with regions of poor conformity. This could be because the action of pressing on a sleeve plastically smoothes out long wavelength roughness leading to a more conforming surface.

Key words: press fit, shrink fit, interface pressure, interference fit, contact pressure measurement, ultrasonic reflection, real area of contact

1 INTRODUCTION

Interference fits, where a bush is shrunk or pressed onto a shaft, are common machine components, particularly in the power generation and transmission industries. They represent a flexible and cost effective method for joining components having cylindrical symmetry, dispensing with the need for welded or bolted joints.

The strength of the interference fit assembly depends on the shaft and bush dimensions. The interface must be sufficient such that the force or torque required to cause slip are not reached during normal service. However, in excessive interferences component damage can occur during assembly or high levels of residual stress will be evident.

For example, railway wheels are press or shrink fitted onto axles. The diametral interference is typically 0.192mm [1], which is sufficient such that slip does not occur at the interface during normal tractive wheel operation. However, railway axles occasionally fail by fatigue resulting from the alternating rotating bending loading. The site of the fatigue crack initiation is commonly at the location of the press fit. Clearly a method for measuring the contact stress associated with press fits would prove useful both in component inspection and product development. This paper describes a method based on interpreting the reflection of ultrasound at the interface to determine the contact pressure.

2 BACKGROUND

2.1 Interface Pressure Calculation

The classical method for relating the degree of geometrical overlap in a fit to the resulting contact pressure is given by the theory of Lamé (see for example [2]). The analysis is based on equilibrium of stress and displacement in thick infinitely long cylinders.

The approach yields an expression for the interface pressure, p in terms of the internal bush radius r_1, and the external radius r_2:

$$p = \frac{E\left(r_2{}^2 - r_1{}^2\right)}{4r_1 r_2{}^2} I \tag{1}$$

where I is the diametral interference (i.e. overlap of the shaft and bush) and E is the Young's modulus.

The Lamé solution is limited by its basic assumptions. The approach will not predict the stress concentrations at the ends of the joint and nor is it suitable for a bush of changing section (a railway wheel for example). Generally numerical methods, principally finite or boundary element analysis, are used to determine contact stress distribution [3, 4, 5, 6, 7]. These methods can be used to predict non-uniform contact pressures at the interface caused by geometry changes and edge stress discontinuities.

2.2 Ultrasonic Reflection from an Interface

A wave of ultrasound will be reflected back from an interface between two materials. The proportion of the wave reflected depends on the relative acoustic impedance (i.e. the product of the density and the sound velocity) of the two materials. The ratio of the amplitude of the reflected wave, A_r, to the amplitude of the incident wave, A_i, known as the *reflection coefficient*, R, is determined by:

$$R = \frac{A_r}{A_i} = \frac{z_1 - z_2}{z_1 + z_2} \tag{2}$$

where z is the acoustic impedance of the media and the subscripts refer to the two sides of the interface. If a wave is travelling through steel and is incident at an air interface then virtually all the wave will be reflected (since the acoustic mismatch is large, $z_1 \gg z_2$). Conversely, if the wave strikes a steel-steel interface and there is perfect contact then it will be fully transmitted ($z_1 = z_2$).

However, surfaces are always rough to some extent and pressing them together results in contact at the asperities. The interface thus consists of regimes of contact separated by air

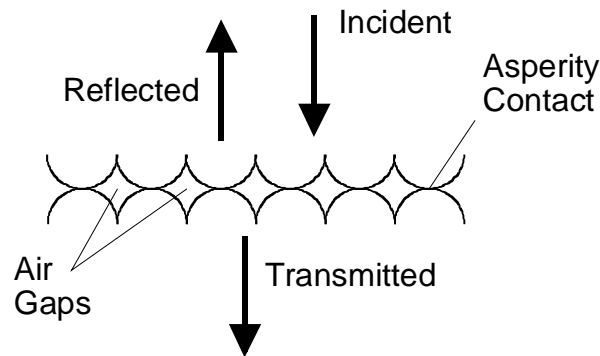gaps. Therefore, a wave incident at a rough surface contact will be partially reflected (see Figure 1).

Figure 1. Partial Reflection of Ultrasound at a Rough Surface Contact

If the wavelength of the ultrasound is large compared with the size of the air gaps then the response of the interface can be determined using a quasi-static spring model [8]. The interface behaves like a flexible spring in between two stiff springs corresponding to the bodies. The reflection coefficient depends on the stiffness of the interface spring, K according to:

$$R = \frac{z_1 - z_2 + i\omega(z_1 z_2 / K)}{z_1 + z_2 + i\omega(z_1 z_2 / K)} \qquad (3)$$

If the materials either side of the interface are identical then this reduces to:

$$|R| = \frac{1}{\sqrt{1 + (2K / \omega z)}} \qquad (4)$$

where ω is the angular frequency (= $2\pi f$) of the ultrasound wave. It has been demonstrated that typical engineering rough surface contacts were sensitive to ultrasound frequencies in the regime 1 – 50MHz; and that the reflection of ultrasound could be used to determine information about the nature of the contact at an interface [9].

The stiffness of a dry interface, K (expressed per unit area) is the load required to cause unit approach of the mean lines of the surface roughness [10]:

$$K = -\frac{\mathrm{d}p}{\mathrm{d}u} \qquad (5)$$

where p is the nominal contact pressure at the interface (i.e. the applied load divided by the apparent geometrical contact area) and u is the separation of the mean lines of the roughness. Thus, as the load on an interface is increased, the surfaces are pressed into closer conformity and the stiffness increases (see Figure 2). The stiffness will vary from zero, when there is vanishingly small contact, to infinity, when the surfaces are completely conformed.
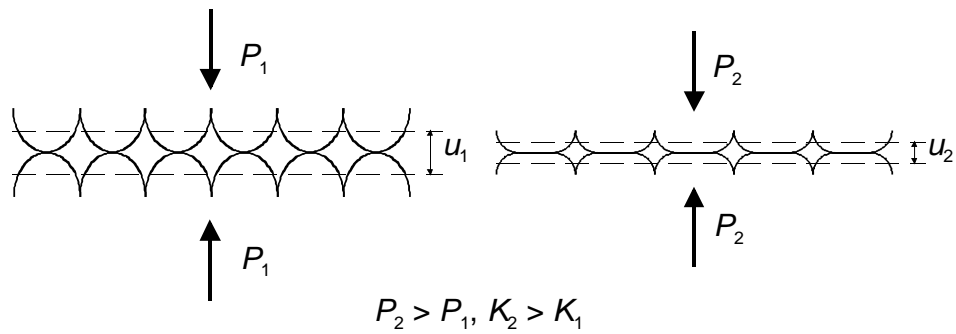
Figure 2. Increasing Interface Stiffness with Greater Surface Conformity

The stiffness of a rough surface interface depends on the number, size and spacing of the regions of contact. A surface with a certain number and size of distributed contact regions would have a higher stiffness if those regions were closely packed. Therefore, there is no unique relationship between stiffness and contact pressure [11]. However, an independent calibration experiment can be performed to determine the relationship between the contact pressure and interface stiffness (for a given pair of rough surfaces). Measurement of the reflection coefficient can therefore provide a quantitative method to determine the contact pressure by empirical calibration [12].

2.3 Ultrasonic Reflection from an Interference Fit

When a bush is pressed or shrunk onto a shaft, the surfaces either side of the joint will be loaded together. Because these surfaces are rough the interface will reflect ultrasound to some extent and will be amenable to the above analysis. The principle is to mount a transducer on the outer face of the bush and emit an ultrasonic wave. This wave passes through the bush and is partially reflected at the shaft/bush interface. The reflected wave is received by the same transducer.

Other authors have recognised the possibilities of using ultrasound as a non-destructive tool to determine press fit integrity. Measurements have been taken of the reduction in amplitude of a reflected ultrasonic pulse at a series of shrink fits [13]. These indicated there was a reduction in amplitude with more secure fits. A similar approach was carried out with a tapered pin pressed into a bush [14]. Ultrasonically scanning (i.e. a C – scan) the interface showed regions of non-contact (zero interface pressure) but experimental difficulties prevented any quantitative comparisons. It has also been shown that the reduction in amplitude of the reflected wave can be related to the press-in load and load to cause shifting [15]. All these approaches have been qualitative only. As yet, they all rely on Lamé predictions of contact pressure to compare with ultrasonic results. It is the aim of this work to deduce that pressure from experimental results and in doing so, produce a method that is useful in conditions where Lamé's assumptions do not apply.

3 EXPERIMENTAL DETAILS

3.1 Ultrasonic Equipment

A spherical focusing 10MHz transducer is mounted in a water bath (in this case a scanning tank) such that the ultrasonic wave is focused at the shaft/bush interface. Ultrasonic waves are generated and received by an ultrasonic pulse-receiver (UPR). The transducer thus acts in

a pitch-catch mode. The reflected signals are captured on a digital oscilloscope and passed to a PC for processing. A schematic illustrating the set-up of the equipment is shown in Figure 3a.

Figure 3b illustrates the scanning tank used in the experiments. It is controlled via a PC, which enables ultrasonic readings to be taken using a transducer over an area at prescribed intervals. The dimensions and resolution of the scan can be varied and selected according to specimen geometry and the accuracy required. The transducer is moved in the x and y direction automatically using electric stepper motors while scanning. Focusing height adjustment of the transducer is achieved manually.

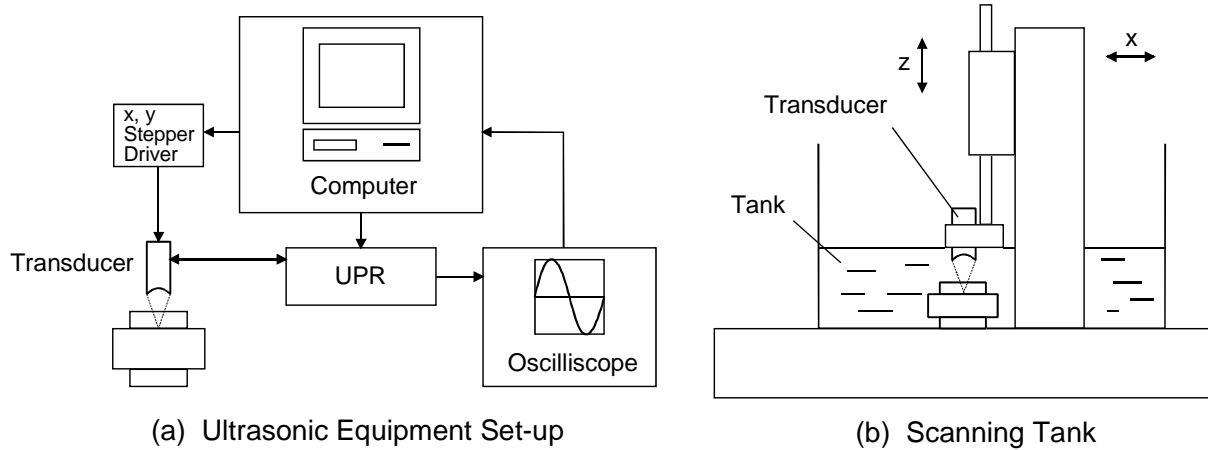(a) Ultrasonic Equipment Set-up   (b) Scanning Tank

Figure 3. Ultrasonic Scanning Apparatus

3.2 Interference Fit Specimens

As shown in Figure 4, the interference fit specimens consisted of a shaft in a sleeve, both of which were manufactured from EN24 steel. The components were lathe finished to a mean surface roughness of 1.5 microns. The hole drilled in each shaft was employed as a reference point for the ultrasonic signal as explained in Section 3.4.
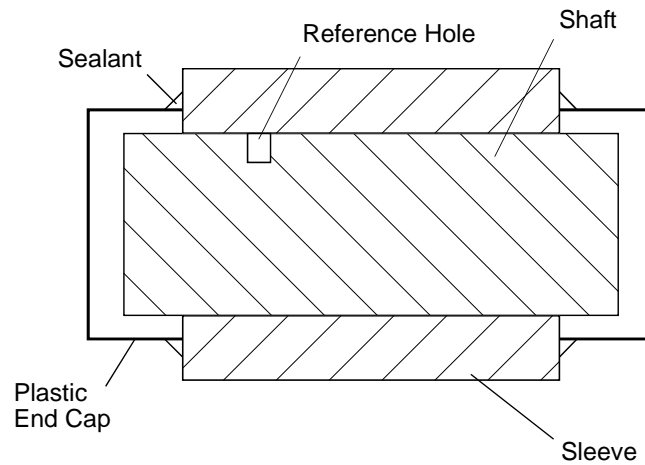
Figure 4. Interference Fit Specimen

The specimens were assembled by press or shrink fitting. Press fitting was performed using a hydraulic press and shrink fitting by cooling the shaft in liquid nitrogen before placing it within the sleeve.

While the ultrasonic measurements were performed the specimens were submerged in water, which acts as a couplant for the ultrasound. Plastic end caps were bonded to the specimen to prevent the water contaminating the interface.

The dimensions of the interference fit specimens examined are shown in Table 1. Dimensions of shafts and sleeves are given as well as interferences. All but one of the specimens were assembled without lubrication.

Table 1. Interference Fit Specimen Geometries

| Diametral Interference (mm) | Assembly Method | Shaft | | Sleeve | | | Shape Factor |
		O.D. (mm)	Length (mm)	I.D. (mm)	O.D. (mm)	Length (mm)	
0.025	Press Fit	50	120	49.975	80	90	6.09
0.050	Press Fit	50	120	49.950	80	90	12.19
0.075	Press Fit	50	120	49.925	80	90	18.28
0.030	Press Fit	50	70	39.970	60	50	8.33
0.030	Shrink Fit	50	70	39.970	60	50	8.33
0.030	Press Fit*	50	30	39.970	60	20	8.33

* press fit carried out with oil lubrication

Due to material and assembly constraints the 0.03mm fit specimens were made to different dimensions. This meant a means of comparison with the larger specimens was required. Examination of Equation 1, relating contact pressure to specimen geometry, revealed that a *shape factor* could be defined which would allow comparison of different shaped specimens:

$$shape\,factor = \frac{I\left(r_2^2 - r_1^2\right)}{r_1 r_2^2} \qquad (6)$$

The shape factor for a typical railway wheel hub/axle interference fit would be approximately 13, which is comparable with the interference fit specimens used in the experiments indicating the relevance of this study.

3.3 Experimental Procedure

The interference fit specimens were placed on a vee block within the scanning tank and the transducer height set-up to scan the sleeve/shaft interface. The transducer is spherically focusing with a focal length of 75mm in water. The wave is refracted at the water/steel interface. The position of the transducer to focus on the interference interface is determined using Snell's law (see Figure 5). In practice the position of the transducer can be determined by monitoring the amplitude of the signal reflected from the interface. The transducer is moved vertically until the amplitude is at a maximum, which will correspond to the probe being in focus.
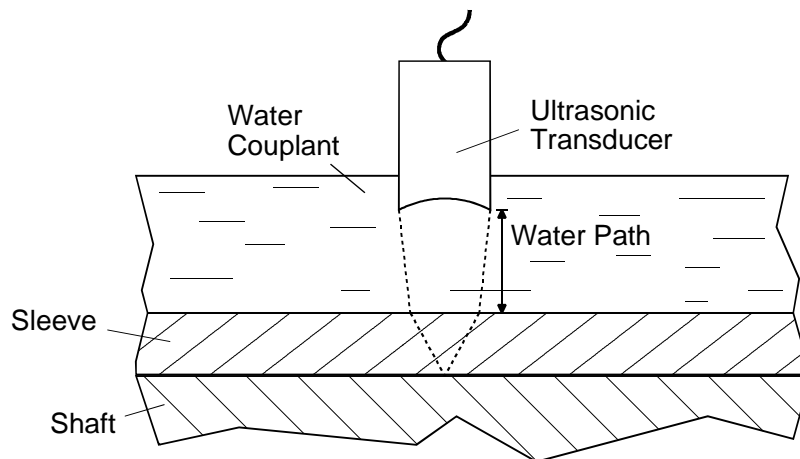

Figure 5. An Ultrasonic Pulse Focused on an Interface

Line scans were taken along the length of each specimen at 10 degree intervals and reflected pulses recorded in order to build up a map of the fit. The specimen was rotated in the vee block after each line scan.

3.4 Signal Processing

Before assembly of the interference fit specimens a reference line scan was taken using the sleeve alone. The reference scan for the small specimens is shown in Figure 6. Away from the edges of the sleeve the reflected pulse is equal to the incident signal, A_i, as it is reflected from a steel-air interface. The decrease in the reflected signal at the edges of the sleeve occurs because as the probe travels over the edge of the sleeve some of the signal is lost (as

shown in Figure 7). This leads to a reduced ultrasonic signal incident on the interface in this region giving a decreased reflected voltage. The amount of signal lost is dependent on the sleeve geometry so another reference scan was carried out for the larger specimens. All subsequent reflected pulses, A_r, from the line scans taken on the assembled interference fit specimens, are divided by the reference scans to give reflection coefficients (as in Equation 2). The reference holes drilled in each shaft were used to check the reference value as the assembled specimens were scanned.
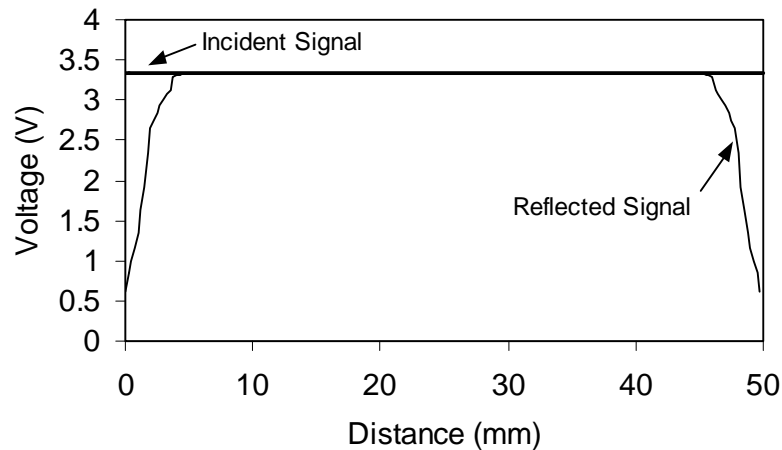

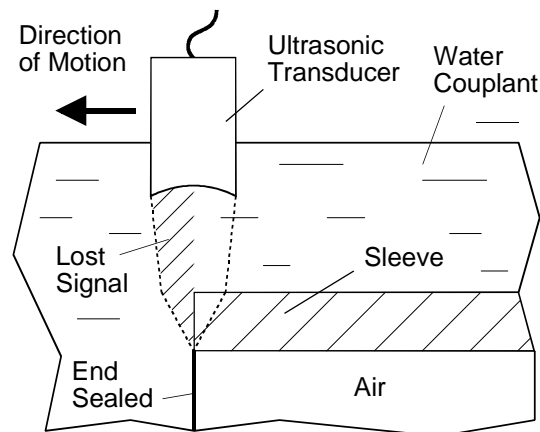Figure 6. Reference Line Scan for the Smaller Specimen Geometry

Figure 7. Incident Signal Loss at the Edge of the Sleeve

The incident pulse used consists of a broad band of frequencies, each of which will be reflected back from the interface according to Equation 4. An example reflected pulse is shown in Figure 8a. For this transducer, useful energy is obtained in the bandwidth 6.5 to 11MHz. This is then divided by the reference pulse spectra to give the reflection coefficient spectra (Figure 8b). The reflection coefficient is clearly frequency dependent. Application of the spring model (Equation 4) gives the stiffness of the interface (Figure 8c). Clearly, whilst the reflection coefficient recorded at a single location on the interface is a function of frequency, the stiffness at that location should be frequency independent. The data shown in Figure 8c demonstrates that the stiffness calculated does not vary with the frequency of the wave used in its measurement. This provides an independent check that the spring model assumptions, of large wavelength with respect to gap size, are valid in this case.
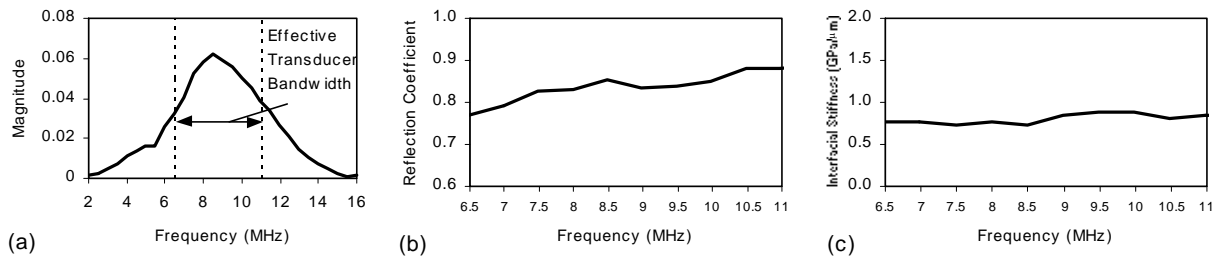
Figure 8. Spectra of (a) Reflected Ultrasonic Pulse; (b) Reflection Coefficient and (c) Interfacial Stiffness, Recorded at a Single Location on an Interference Fit of $I = 0.025$mm

The stiffness of the interface cannot be uniquely related to the real area of contact or the contact pressure. The stiffness depends on the number and size of the regions of asperity contact and also on their distribution. So whilst this analysis can provide qualitative information about the interface it will not provide the interface pressure. For this, an independent method to relate R (or K) to pressure is needed. The incorporation of some kind of contact model (which includes a distribution of asperity contacts) can be used, but the predictions of these models have tended, in the past, to give only marginal agreement with ultrasonic measurements [9]. For this work an experimental calibration approach has been chosen to relate reflection to contact pressure.

3.5 Independent Calibration Experiment

Figure 9 shows the apparatus used for determining the relationship between stiffness and contact pressure.
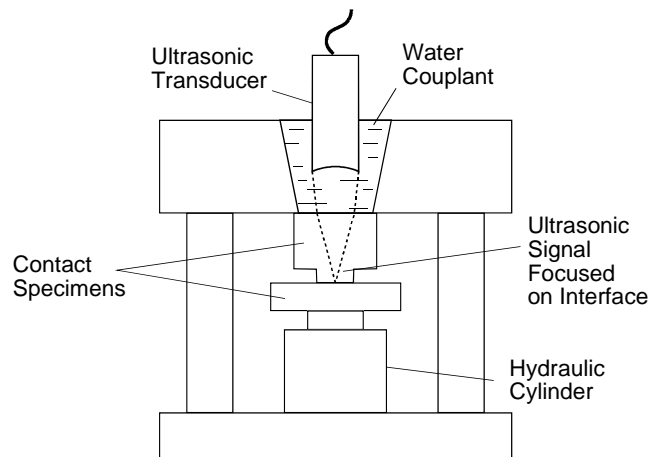

Figure 9. Calibration Apparatus

Two specimens were manufactured from EN24. The contact faces were machined using the same manner as the interference fit specimens to ensure that the roughness was as close as possible to that of the shaft and sleeve contact surfaces. The specimens were loaded together hydraulically. An ultrasonic signal was then focused on the interface between the two specimens. The reflected signal was divided by a reference signal, obtained by recording the reflected pulse when the interface was unloaded, to obtain a reflection coefficient. This was then converted to an interfacial stiffness using the spring model (Equation 4). Stiffness was calculated for a number of different loads to generate a calibration curve (see Figure 10).
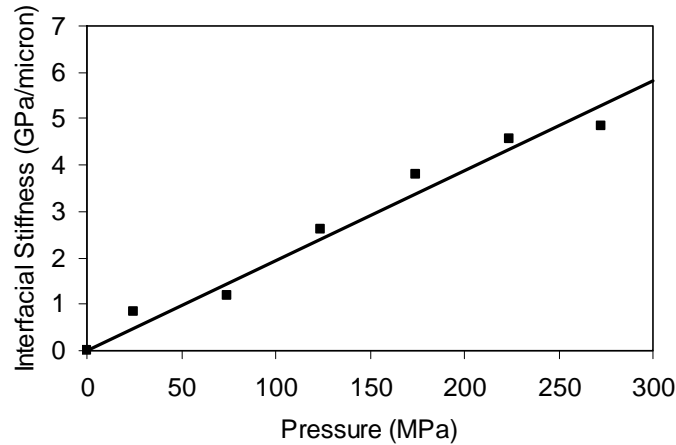
Figure 10. Interfacial Stiffness/Contact Pressure Calibration

The equation for the best fit line through the experimental data is given by $p = 51.72K$. It relates contact pressure, p, to interfacial stiffness, K, and was used to process stiffness data for the interference fit specimens in this series of experiments.

At these relatively low pressures the relationship between stiffness and pressure is close to linear. At higher loads, where more surface conformity occurs, the slope increases as the stiffness tends to infinity. It would therefore be unacceptable to use this relationship for pressures significantly outside the calibration test range or indeed for any other material or rough surface combination. This curve is the first loading on the pair of machined surfaces. Some of this loading takes place plastically and subsequent unloading and re-loading lines do not follow the same path (see [16]) for more detailed work on loading cycles). It is appropriate to use this first loading as a calibration for an interference fit which is assembled for the first time.

4 RESULTS

4.1 Pressure Maps

Reflection scans were recorded for each of the interference fit specimens. Figure 11 illustrates scans for the 0.025mm, 0.05mm and 0.075mm fits.

Each reflection coefficient was converted to a stiffness using the spring model. A check was made on the stiffness data to ensure that stiffness does not vary with the ultrasonic frequency (as described in Section 3.4). Then the calibration plot (Figure 10) was used to produce pressure maps.
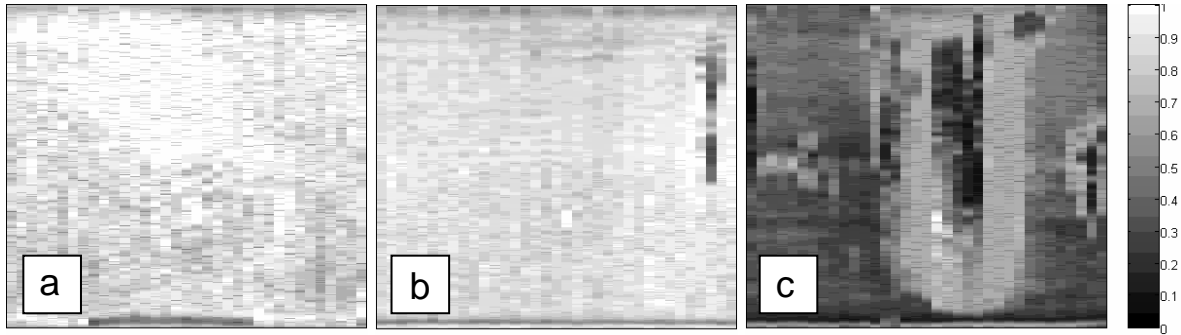
Figure 11. Reflection Coefficient Maps for (a) the 0.025mm Fit; (b) the 0.05mm Fit and (c) the 0.075mm Fit

Figure 12 shows pressure map for the 0.025mm, 0.05mm and 0.075mm fits. As can be seen, the contact pressure along the length of the interfaces is not constant. However, as may be expected there was a high degree of radial symmetry. Each of the plots shows a central region of approximately constant pressure with an increase in pressure at the edges of the interface. In the 0.05mm and 0.075mm fits anomalies occurred (such as highlighted in Figures 12b and c and also apparent on the *R* plots shown in Figure 11), where higher than expected pressures were evident.
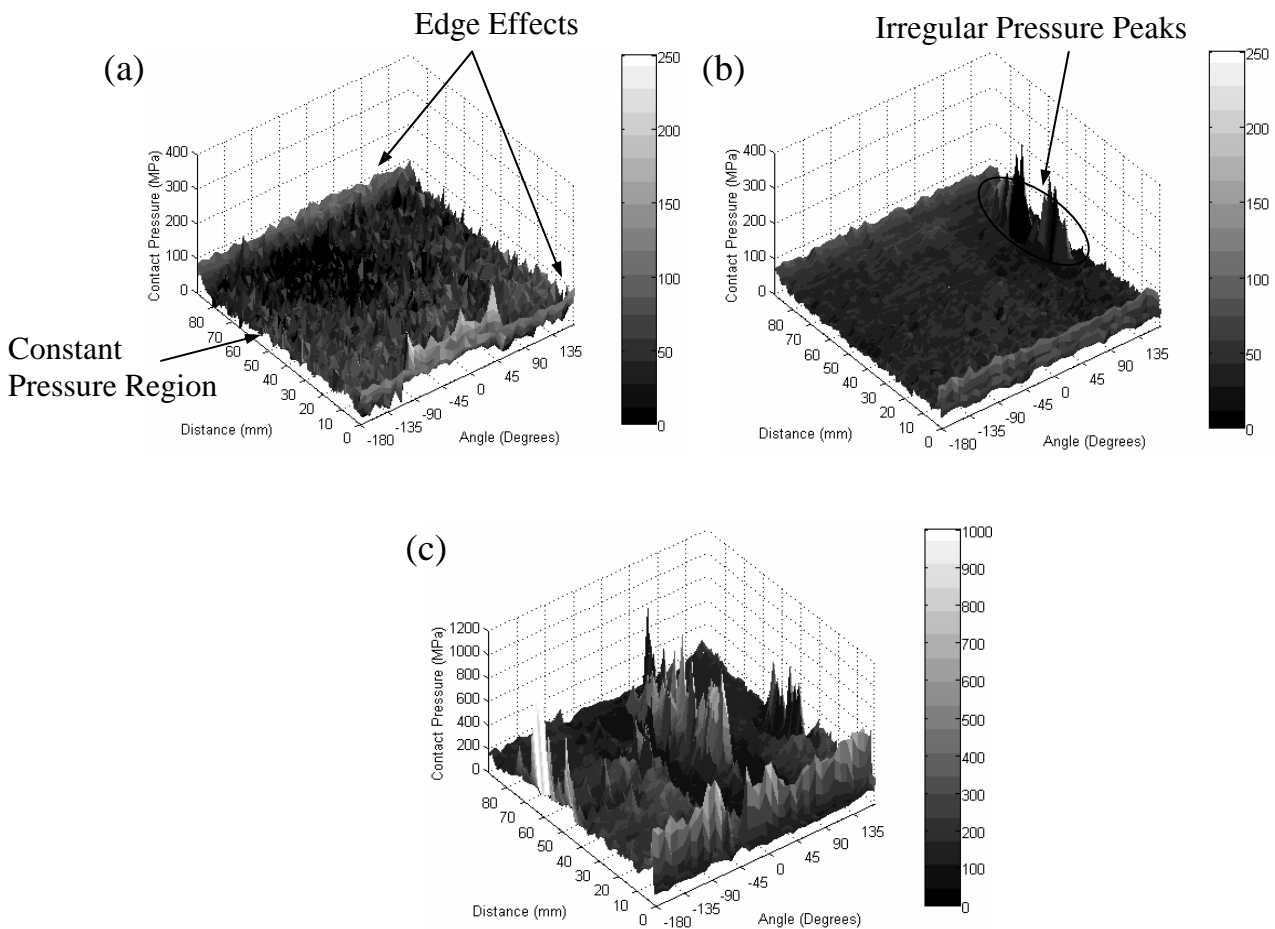

Figure 12. Contact Pressure Map for (a) the 0.025 mm Fit; (b) the 0.05mm Fit and (c) the 0.075mm Fit

Figure 13 shows pressures profiles along the length of the 0.025, 0.05 and 0.075mm interference fit specimens. As the interference increases the contact pressure increases. Variation in the pressure is apparent within the plateau regions. This is probably caused by the variability in the surface roughness across the interfaces.

The marked rises in contact pressure at the edges of the interference fits occurred for all the specimens. Classical solid mechanics theories (see for example [2]) associate a stress-raising factor to an edge. Therefore, the occurrence of edge effects within the ultrasound measurements of interface contact pressure is both expected and reasonable.

As can be seen in Figure 13 the contact pressure decreases again before the edge of each fit. In order to try and explain this surface profiles were taken of the 0.075mm fit sleeve edges. It could be seen that at the edges the profile dropped away (see Figure 14). The drop-off causes a reduction in the interference and therefore the stress raising effect. At the left side the drop-off is smaller and so a pressure increase occurs before the edge, on the right hand side a larger drop-off occurs which explains the absence of a pressure increase. The drop-off was thought to be due to discrepencies in the manufacturing process.
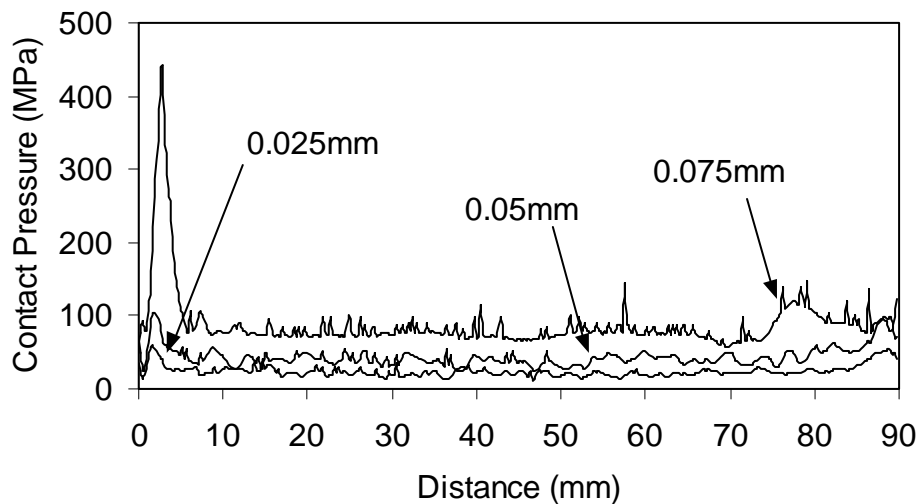
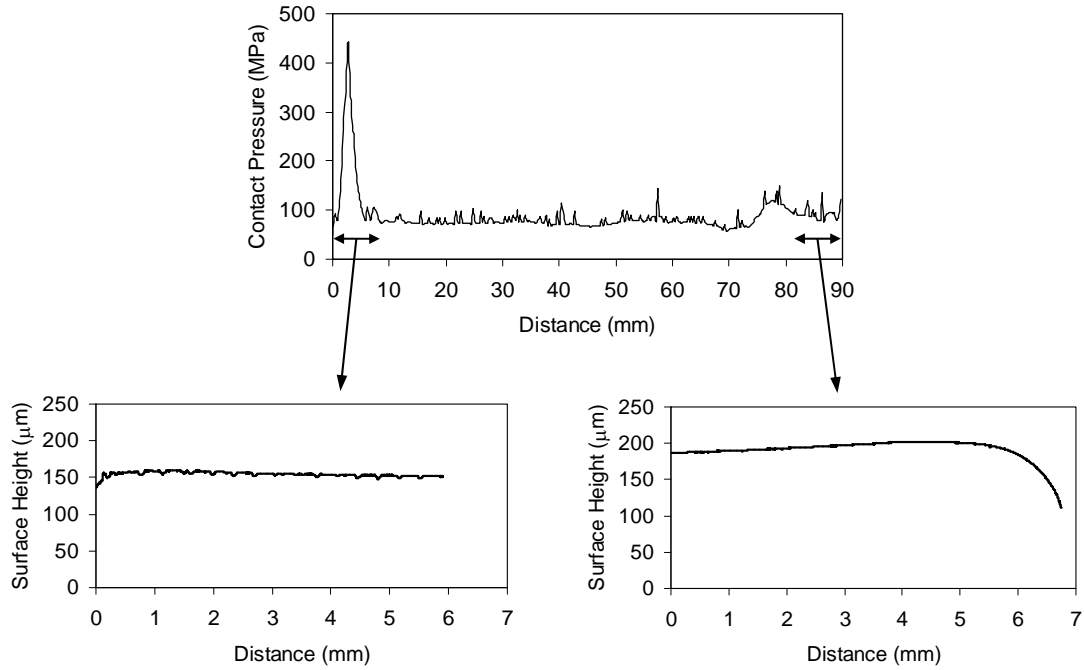Figure 13. Line Scans of the 0.025, 0.05, and 0.075mm Fits

Figure 14. Profiles of the 0.075mm Fit Sleeve Edges

The contact pressures recorded for the specimens can be compared to the Lamé predictions. Figure 15 shows plots of predicted interface pressure (by thick cylinder analysis, Equation 1) against the shape factor defined by Equation 6 (incorporating diametral interference and sleeve I.D. and O.D.). The average contact pressure over the central part of the fit (neglecting the edge peaks), determined from the ultrasound results, are plotted on the same axes. There is good correlation between the experimental results and Lamé predictions.
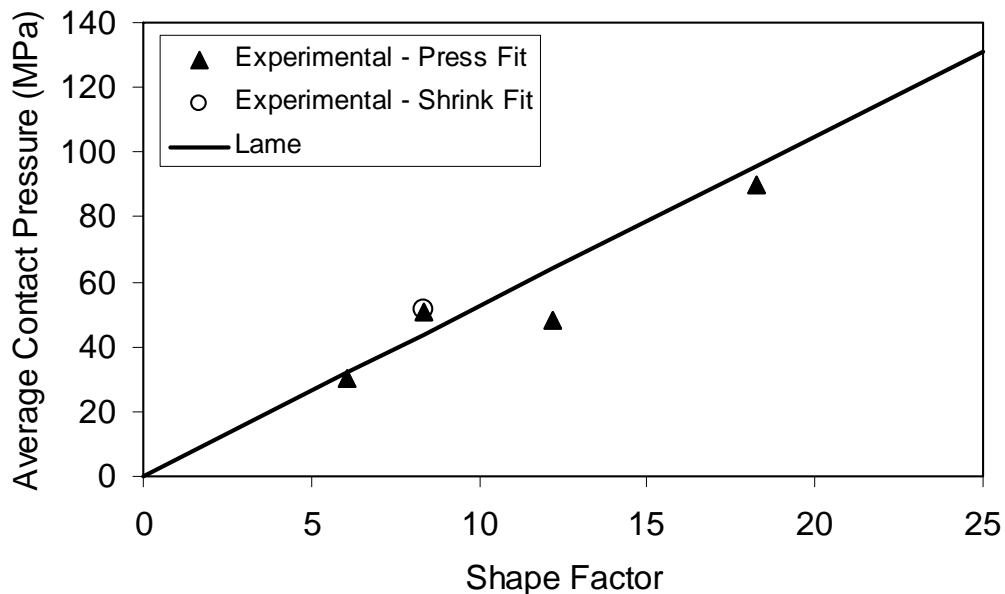

Figure 15. Comparison of Average Measured Pressure (excluding edge effects) and Theoretical Interface Pressure Determined from Lamé Analysis

4.2 Anomalies and Surface Damage

Low reflection coefficients were also seen in the irregular pressure peak regions seen away from the edge effects on the 0.05mm and 0.075mm fit pressure plots. A check on the 0.05mm fit stiffness data indicated that it was not independent of frequency in the anomaly area (see Figure 16). This indicates that the surface in this region is very rough and therefore the low reflection coefficients seen are as a result of ultrasound being scattered rather than more being transmitted due to high contact pressures.

After the experimental readings had been taken the interference fit specimens were cut open. Upon visual inspection of the interface, it was found that for all the specimens an anomaly in the pressure and reflection coefficient maps corresponded to surface damage and hence greater roughness. It should be noted that surface damage on the shaft of the interference fit was mirrored on the sleeve. Figure 17a shows a photograph of the surface of the shaft from the 0.075mm interference fit specimen. Comparison of this image with the corresponding reflection coefficient map (Figure 17b) indicates that the surface damage clearly corresponds to the anomalies.
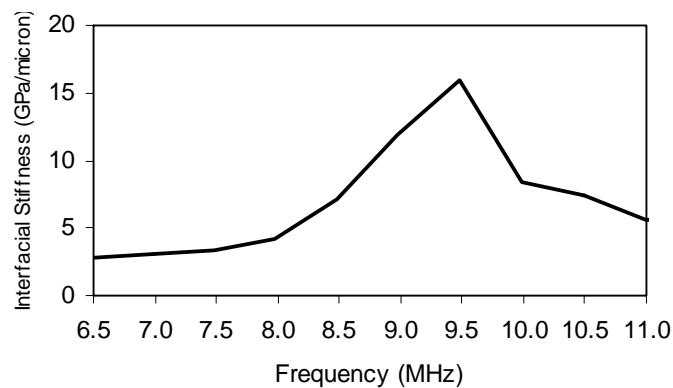

Figure 16. Interfacial Stiffness vs Frequency for 0.05mm Fit Anomaly Region

The anomalies were therefore not caused by pressure increases, but attributable to surface damage scattering the signal. The surface damage was only observed for the 0.05mm and 0.075mm specimens. A relatively high load was required to press fit these specimens, which was clearly high enough to lead to localised seizure and subsequent surface damage on the shafts and sleeves.
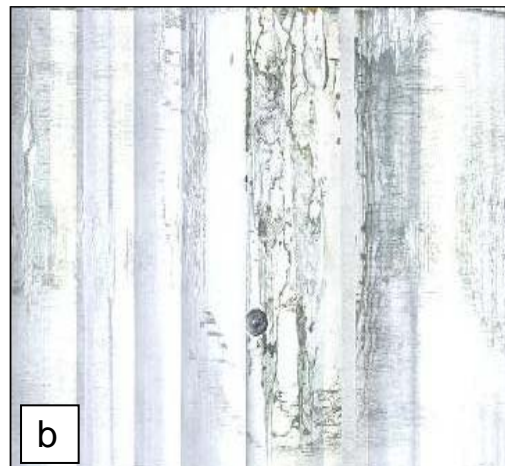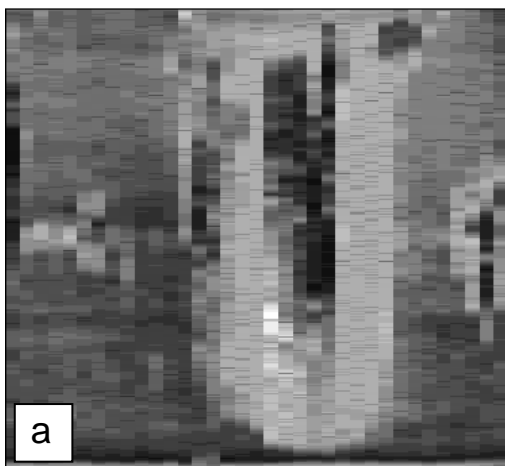
Figure 17. 0.075mm Fit (a) Reflection Coefficient Map; (b) Photograph of Shaft Surface

4.3 Shrink Fitting versus Press Fitting

The two specimens of 0.03mm interference had identical radial dimensions. However, one of the specimens was shrink fitted and the other press fitted. It was found that the edge effects for each specimen were of similar magnitude, and the average pressures neglecting these were almost identical (see Figure 18). Within the interface of the press fitted specimen the contact was relatively uniform. However, for the shrink fitted specimen there were large areas where the shaft/sleeve contact was minimal.
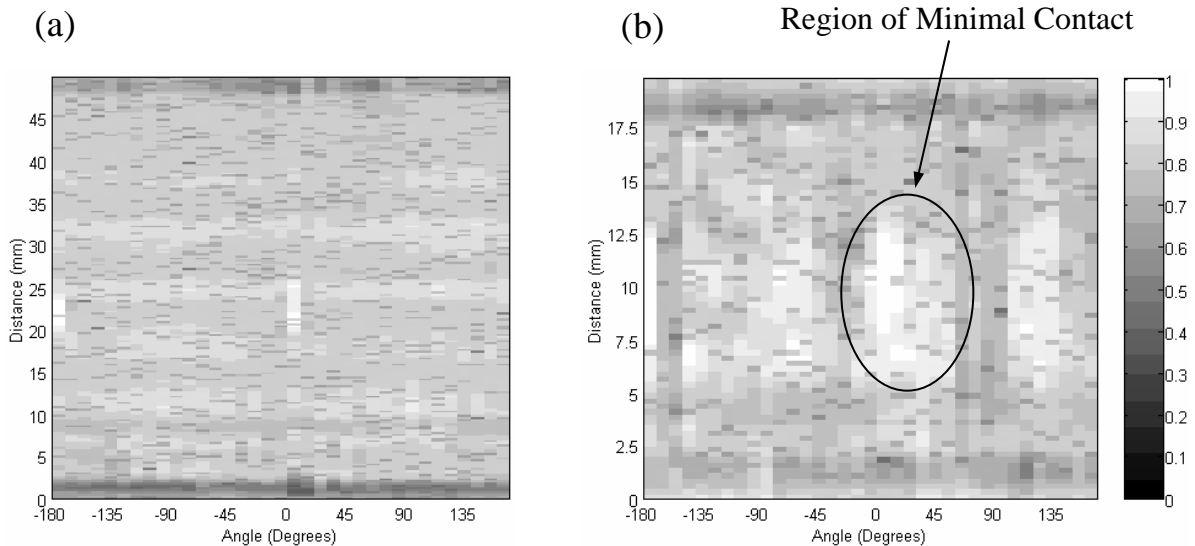
(a)

(b)

Region of Minimal Contact

Figure 18. Reflection Coefficient Maps of (a) 0.03 mm Press Fit and (b) 0.03mm Shrink Fit

These regions become clearer when studying the pressure profiles. Figure 19 illustrates shrink fit pressure profiles for regions of *good* and *poor* contact (taken at -160° and 10° respectively (see Figure 18b)).
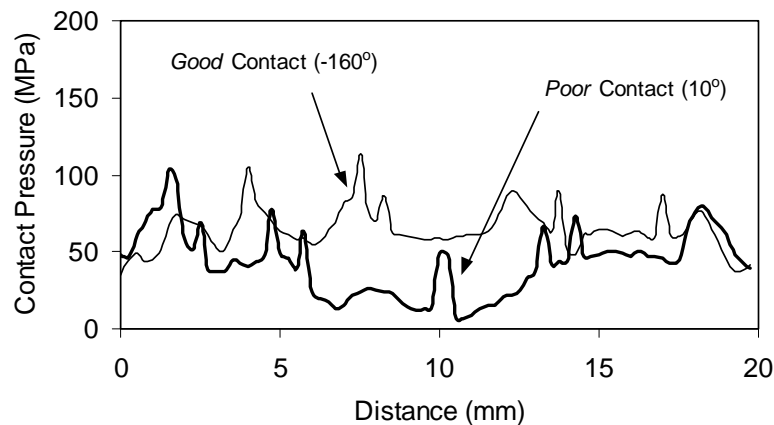
Figure 19. Shrink Fit Pressure Profiles for Good and Poor Contact (-160° and 10° respectively (see Figure 15b))

The trends shown at the two interfaces can be explained by considering the different methods of assembly. When press fitting, the surfaces of the shaft and sleeve push past one another.

The surfaces plastically deform, removing any waviness in their topography, leading to a uniform contact. In shrink fitting the surfaces come together as the shaft expands, instead of sliding against each other. Hence, when shrink fitting an interference fit the contacting surfaces do not conform as much at the interface, leading to variations in the intensity of the contact.

Surface damage may occur when press fitting due to the surface interactions. Such damage cannot occur for shrink fitted specimens.

4.5 Lubrication of the Interface

An experiment was performed to investigate whether the presence of a lubricant inhibited ultrasonic characterisation of an interference fit. Lubricants are often used when assembling interference fits, and may remain in the interface afterward. A 0.03 mm fit was constructed using a mineral oil to provide lubrication during the press fitting operation. After scanning, the specimen was cut open. Visual inspection revealed that a film of oil was still present on the interface.
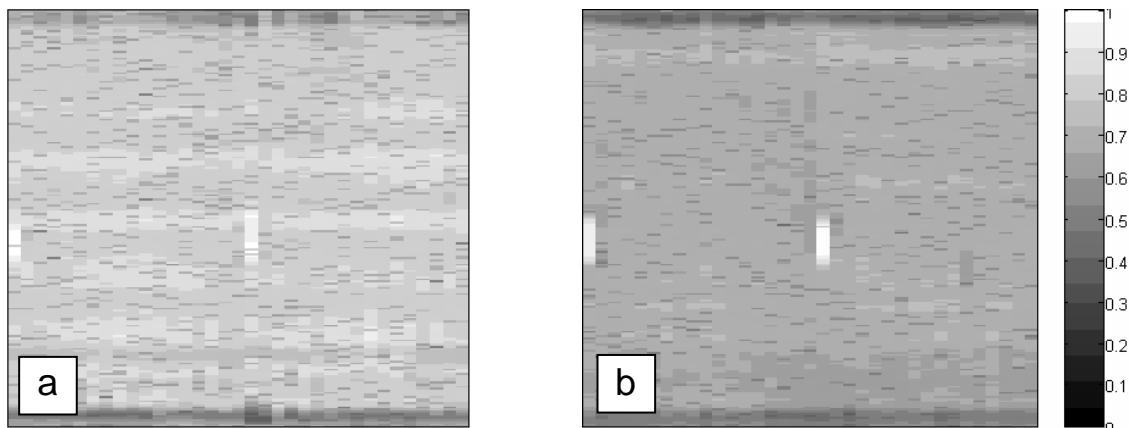

Figure 20. Reflection Coefficient Maps of 0.03 mm Press Fit (a) Dry and (b) Lubricated

As can be seen in Figure 20b, lubricant in the interface did not inhibit measurement of reflected ultrasound. The reflection coefficient did reduce, however, from an average value of 0.804 for the dry specimen to 0.644 for the lubricated case. Transmission of ultrasound has therefore been increased. This result is not unexpected since the oil occupies the interface areas once filled with air, and due to its lower impedance than air, transmits more of the ultrasonic signal. The increased ultrasonic transmission means the previous calibration performed is not applicable to the lubricated interface; hence, the contact pressure map cannot be constructed.

The transmission of ultrasound through a mixed solid-solid, solid-liquid-solid interface is a more complex problem. A spring model approach can still be used (equation 4 – Rog can you check the number) but now the interface stiffness is the stiffness of the solid part and of the liquid part in parallel. A calibration route could be used to determine the effect of the liquid (using surfaces coated with oil), but this could be very dependent on the thickness of the oil layer. Alternatively it has been shown in [18] that the liquid stiffnesses is given by:

$$K = \frac{\rho c^2}{u} \qquad (7)$$

and that this can be deduced from the solid stiffness (equation 5). This enables the combined stiffness to be separated into its liquid and solid parts. Whilst this method has not been fully evaluated for a practical case such as the work presented here; it could potentially be a route to interpreting reflection maps from mixed liquid-solid contacts.

5 DISCUSSION

The contact between the surface of a shaft and the inner bore of a bush are inherently rough. This permits the possibility of using ultrasound to determine the interface pressure. It has been demonstrated that for conventional machined surfaces (turned or ground) the method is feasible. But if some kind of surface damage takes place then the surfaces become too rough and the approach breaks down. Then size of the air gaps becomes comparable in size to the ultrasonic wavelength, and incoherent scattering occurs at the interface. Of course, this is an indication that damage has occurred on an otherwise regular surface. Potentially, it is possible to study rougher interfaces by using lower frequency ultrasound; but this has not been explored.

The approach presented here relies on some form of independent calibration being performed. This is unfortunate because the accuracy of the calibration depends on the similarity of the roughness of the specimen contacting surfaces to that of the interference faces. As yet, there is no method to obtain directly the contact pressure, or real area of contact, analytically from measurements of reflection.

The work carried out here has been based on the normal incidence of the ultrasonic wave on the interface. In some applications, it may not be possible to gain such access to the interface. It is possible to direct ultrasonic waves obliquely onto the interface and receive the reflected signal using another transducer (i.e. pitch catch mode) (as described in [17]). It has also been convenient to use immersion transducers to focus and couple through a water path. It would also be feasible to use contact transducers bonded directly to the surface but then it becomes less easy to scan an interface. Moving away from normal incidence immersion problems will inevitably lead to more geometrical problems associated with coupling, focusing, and scanning.

Notwithstanding the above, there is potential for this approach to be used in many press fit applications, both as a tool for non-destructively testing joints and also as an aid to the design and selection of fits. Furthermore, the method could be adapted for use in any contact application provided the surfaces are dry and the interface is relatively large.

6 CONCLUSIONS

(i) A method has been established to determine interface pressures in a press fit component. The method relies on the measurement of reflected ultrasonic wave and a parallel calibration procedure.

(ii) The spectrum of the reflected pulse is analysed using a spring model to determine the stiffness of the interface. In the region of the press fit the stiffness of the interface does not vary with ultrasonic frequency indicating the validity of this quasi-static model.

(iii) The interface contact pressure has been determined for a number of different press and shrink fit cases. The results show a central region of approximately uniform

pressure with edge stress at the contact sides. The magnitude of the pressure in the central region agrees well with the elastic Lamé analysis.

(iv)   In the more severe press fit cases, the surfaces scuffed which lead to anomalies in the reflected ultrasound. These anomalies were associated with regions of surface damage at the interface.

(v)   The average contact pressure in a shrink fit and press fit joint were similar. However in the shrink fit joint more uneven contact pressure was observed with regions of poor conformity. Possibly the action of pressing, in contrast to shrinking, on a sleeve plastically smoothes out long wavelength roughness leading to a more conforming surface.

(vi)   The principle limitations of this approach are: separate calibrations are required to establish the effect of changing geometry at the edges of the fits and also to obtain contact pressure directly from reflection and the presence of a lubricant or other contaminant at the interface upsets the results.

7 REFERENCES

[1]   pr EN 13260, 1998, "Railway Application - Wheelsets and Bogies - Wheelsets - Product Requirement".

[2]   Boresi, A.P., Schmidt, R.J., Sidebottom, O.M., 1952, *Advanced Mechanics of Materials*, Wiley.

[3]   Zhao, H., 1997, "Numerical Analysis of the Interference Fitting Stresses Between Wheel and Shaft", *International Journal of Materials and Product Technology*, Vol. 12, Nos 4-6, pp514-526.

[4]   Garnett, M.D., Grimm, T.R., 1989, "Finite Element Analysis of Interference Fitted Shafts Subjected to Bending", *Proceedings of the ASME International Conference on Computers in Engineering*, Anaheim, USA, 30 July - 3 August, pp272-280.

[5]   Karami, G., Oskooei, S.G., 1994, "Boundary Element Analysis of Shrink-Fit Type Problems", *Proceedings of the 2nd Biennial European Joint Conference on Engineering Systems Design and Analysis*, Vol. 8A, London, England, 4-7 July, pp17-21.

[6]   Yang, G.M., Coquille, J.C., Fontaine, J.F., Lambertin, M., 2001, "Influence of Roughness on Characteristics of Tight Interference Fit of a Shaft and a Hub", *International Journal of Solids and Structures*, Vol. 38, pp7691-7701.

[7]   Zhang, Y., McClain, B., Fang, X.D., 2000, "Design of Interference Fits Via Finite Element Method", *International Journal of Mechanical Sciences*, Vol. 42, pp1835-1850.

[8]   Tattersall, A.G., 1973, "The Ultrasonic Pulse-Echo Technique as Applied to Adhesion Testing", *J. Phys. D: Appl. Phys*, Vol. 6, pp819-832.

[9]   Drinkwater, B.W., Dwyer-Joyce, R.S., Cawley, P., 1996, "A Study of the Interaction between Ultrasound and a Partially Contacting Solid-Solid Interface", *Proceedings of the Royal Society Series A*, Vol. 452, No. 1955, pp. 2613-2628.

[10]   Thomas, T.R. Sayles, R.S., 1977, "Stiffness of Machine Tool Joints: A Random-Process Approach", *Trans. ASME, J. Eng. Ind.*, Paper No. 76-WA/Prod-23.

[11]   Kendall, K. and Tabor, D., 1971, An Ultrasonic Study of the Area of Contact between Stationary and Sliding Surfaces", *Proceedings of the Royal Society, Series A*, Vol. 323, pp321-340.

[12]   Dwyer-Joyce, R.S., Drinkwater, B.W., 1998, "Analysis of Contact Pressure Using Ultrasonic Reflection", *Experimental Mechanics*, *Proceedings of the 11th International Conference on Experimental Mechanics*, Balkema, Rotterdam, pp747-754.

[13]   Tsao, M.C., Grills, R.H., Simpson, R.P., Andrew, G.A., 1984, "Ultrasonic Colour Imaging and Stress Analysis of Piping Coupler Shrink Fit", *Materials Evaluation*, Vol. 42, pp1393-1400.

[14]   Mott, G., Taszarek, B.J., 1985, "Ultrasonic Characterisation of an Interference Fit", *Materials Evaluation*, Vol. 43, pp990-994.

[15]   Bergner, F., Bersch, H., Binger, G., Jungnickel, W., Wolf, A., 1998, "Ultrasonic Testing of Longitudinal Press Fits", Materialprufung, Vol. 40, No 5, pp177-181.

[16]   Dwyer-Joyce, R.S., Drinkwater, B.W., Quinn, A.M., 2001, "The Use of Ultrasound in the Investigation of Rough Surface Interfaces", *ASME Journal of Tribology*, Vol. 123, pp8-16.

[17]   Baltazar, A., Rokhlin, S., Pecorari, C., 2002, "On the Relationship between Ultrasonic and Micromechanical Properties of Contacting Rough Surfaces", *Journal of the Mechanics and Physics of Solids*, Vol. 50, pp1397-1416.

[18]   Gonzalez-Valadez, M. and Dwyer-Joyce, R.S., (2004), "Ultrasound and Mixed Liquid-Solid Contacts", Proceedings of the 31th Leeds-Lyon Symposium on Tribology, in press.